Metagenomic and lipid analyses reveal a diel cycle in a hypersaline microbial ecosystem

Supplemental Documents

Table of Contents

Supplemental Methods 1.

S1.1 Core Lipid Saponification and Identification

Core lipid concentrations were measured by GC-FID after alkaline saponification of the microbial biomass (Table 2). Quantification of saponified whole cell lipids was achieved on an Agilent 6890 GC-FID system using a high temperature capillary column (J&W Agilent Technologies, Santa Clara, CA, USA, DB-5HT, 30 m length, 0.25 mm inner diameter, 0.1 μm film thickness) with helium as carrier gas (constant flow). The GC oven was programmed from 60 °C (2 min) to 350 °C at a rate of 4 °C min^{-1}, followed by an isothermal phase of 20 min. The injector temperature was programmed from 60 °C (5 s) to 350°C (60 s) at 10°C s^{-1}. Behenic acid methyl ester was used as internal standard.

The TMS and methylester derivates were identified by GC-MS in full scan mode using an Agilent 6890N gas chromatograph (Agilent Technologies, Santa Clara, CA, United States) equipped with a DB-5 column (60 m, 0.25 mm, 0.25 μm film thickness, Agilent J&W Agilent Technologies, Santa Clara, CA, USA) with helium as carrier gas (constant flow). The GC oven was programmed from 40°C (2 min) to 315°C at a rate of 4°C min^{-1}, followed by an isothermal phase of 50 min. The injector temperature was programmed from 40°C (5 s) to 315°C (60 s) at 10°C s^{-1}. The gas chromatograph was coupled to an AutoSpec Premier sector field mass spectrometer (Micromass MS Technologies, Manchester, UK, mass range: 55 - 600 da) run at an electron impact ionization energy (EI) of 70 eV and source temperature of 260°C. Compounds were identified using retention times and mass spectra in comparison to commercial available standards.

S1.2 Core lipid quantification errors

To determine the quantification error using GC-FID, we performed repeat-injection experiments (up to four times) of selected samples. The determined average standard deviation for FA and archaeol quantification was 2.6% and the range 0.2% for the highest concentrated lipid (DPG) to 7% for less abundant compounds. We also split three samples into three batches each and derivatized them separately. The resulting average

standard deviation for absolute compound concentrations, including derivatisation and integration errors, was 4.1%.

S1.3 Intact polar lipids (IPLs)

To assess the presence of lipids that are not GC-MS amenable such as GDGTs that would distort bacterial/archaeal abundance measurements based on core lipids, we performed HPLC-MS characterization of the IPL fraction. The only detected core lipid not amenable to GC was halocapnine that occurred as a component of a bacterial sulfonolipid. However, this lipid only occurred in minor concentrations. GDGTs were not detected. Detailed results of the IPL analyses will be reported in a forthcoming manuscript.

S1.3.1 Extraction of IPLs

One quarter of each filter was used for lipid extraction using a modified Bligh and Dyer procedure (Sturt et al 2004) For the first three extraction steps, the extraction solvent consisted of methanol, dichloromethane and phosphate buffer (8.7 g K_2HPO_4 per liter water) in a composition of 2:1:0.8 (v:v:v). For the following three extraction steps an aqueous solution of trichloroacetic acid (50 g L^{-1} CCl_3COOH) was used for the Bligh-Dyer mixture instead of the phosphate buffer. After sonication for 10 min and centrifugation for 4 min the supernatants were combined in a separation funnel. Dichloromethane and water were added to the mixture to achieve phase separation at a final methanol/dichloromethane/buffer ratio of 1:1:0.8. After removing the organic phase containing the IPLs, the aqueous phase was extracted two more times with dichloromethane. All organic solvents were GC Resolv1 or Optima1 grade (Mallinckrodt, Phillipsburg, NJ, USA); deionized water was obtained from a MilliQ1 system (Millipore, Billerica, MA, USA). To reduce the loss of intact polar lipids prior to analysis via HPLC MS, no separation or cleaning of the extracts was performed.

S1.3.2 HPLC-analysis of IPLs

Extracts were dissolved in Eluent A, and phosphatidylethanolamine glycerol dialkylether (O-PE, Avanti polar lipids, inc., Alabaster, AL, USA) with side chains containing 16 carbon atoms, each) was added as injection standard. Phospholipids were analyzed on an HPLC instrument (Agilent 1100 Series, Agilent Technologies, Santa Clara, CA, USA)

coupled to an LCQ DECA XP ion-trap mass spectrometer (Thermo Finnigan, San Jose, CA, USA) equipped with an electrospray ionization source (ESI). HPLC separation was achieved, as described by Rütters et al. (2001), on a diol phase (LiChrospher100 Diol 5 µ, CS - Chromatographie Service GmbH, Langerwehe, Germany) using a 125 x 3 mm column with 20 mm guard column filled with the same material. A flow rate of 0.2 ml min^{-1} was employed with the following solvent gradient: 1 min 100 % A, increasing over 20 min to 35 % A, 65 % B using a linear gradient, followed by 40 min of reconditioning. Eluent A was a mixture of *n*-hexane, isopropanol, formic acid, ammonia (25 % solution in water) (79:20:1.2:0.04 by volume), eluent B was isopropanol, water, formic acid, ammonia (25 % solution in water) (88:10:1.2:0.04 by volume). The optimal mass spectrometer settings were determined by direct injection of the injection standard O-PE. For negative ion-mode the mass spectrometer was set to a spray voltage of 3 kV, sheath gas flow of 30 (arbitrary units), capillary voltage of -45 V and a capillary temperature of 220°C. For positive ion-mode we observed highest ion intensities with a spray voltage of 3 kV, sheath gas flow of 20 (arbitrary units), capillary voltage of +40 V and a capillary temperature of 200°C. MS/MS experiments were done in the dependent-scan mode, i.e. the most intense quasi-molecular ion species of each full scan was automatically isolated and fragmented up to MS^3. Helium was used as collision gas (relative collision energy: 30 – 60 %, depending on compound). Mass spectra (full scan and MS/MS) were used for compound identification and determination. Confirmation of identified compounds was achieved by determination of accurate masses with a high resolution HPLC-ESI-MS system (2695 separations module coupled to Micromass Q-TOF micro, Waters, Milford, MA, USA) without any HPLC separation.

References

Sturt HF, Summons RE, Smith K, Elvert M & Hinrichs KU (2004) Intact polar membrane lipids in prokaryotes and sediments deciphered by high-performance liquid chromatography/electrospray ionization multistage mass spectrometry - new biomarkers for biogeochemistry and microbial ecology. *Rapid Commun Mass Sp* **18**: 617-628.

Supplemental Methods 2.

2.1 Reconstruction of 16S rRNA sequences and estimation of relative abundance using EMIRGE

As an independent measure of community structure dynamics, the expectation maximization iterative reconstruction of genes from the environment (EMIRGE) method (Miller et al 2011) was used to assemble near-full-length 16S rRNA gene sequences from community genomic sequencing reads. Unassembled metagenome sequence from all filter sizes were initially included in the analysis. As 0.1% of paired end reads were estimated to belong to 16S rRNA genes, samples with 226,000 or less reads were excluded from the analysis, leaving 9 samples (Table S2). A SILVA database (release 108), to which the 16S rRNA sequences of additional published Nanohaloarchaea were added, was used to run EMIRGE on each sample. To estimate relative abundance, unique EMIRGE-assembled 16S rRNA sequences were then combined into a candidate database used for a second modified EMIRGE run with parameters set to allow no merging or splitting (-j 1 and -p 1) of new sequences. This allowed an estimation of relative abundance of each reconstructed sequence in each sample. We used the Ribosomal Database Project (RDP) classifier (Wang et al 2007) for hierarchical taxa assignment at the genus and family OTU classification level, with a confidence threshold for each assignment of at least 80%. The relative abundances of sequences of the same genus or family in a sample were summed. Since published Nanohaloarchaea were not part of the RDP database, we used published Nanohaloarchaeal sequences to identify closely related sequences in the EMIRGE output. Sequences with 95% identity to the published sequences were classified as Nanohaloarchaea. We used the Database Enabled Code for

Ideal Probe Hybridization Employing R (DECIPHER) with default parameters to screen for potential chimeras; none were found (Wright et al 2012).

References

Miller CS, Baker BJ, Thomas BC, Singer SW, Banfield JF (2011). EMIRGE: reconstruction of full-length ribosomal genes from microbial community short read sequencing data. *Genome Biol* **12**.

Sturt HF, Summons RE, Smith K, Elvert M, Hinrichs KU (2004). Intact polar membrane lipids in prokaryotes and sediments deciphered by high-performance liquid chromatography/electrospray ionization multistage mass spectrometry - new biomarkers for biogeochemistry and microbial ecology. *Rapid Commun Mass Sp* **18:** 617-628.

Wang Q, Garrity GM, Tiedje JM, Cole JR (2007). Naive Bayesian classifier for rapid assignment of rRNA sequences into the new bacterial taxonomy. *Appl Environ Microb* **73:** 5261-5267.

Wright ES, Yilmaz LS, Noguera DR (2012). DECIPHER, a Search-Based Approach to Chimera Identification for 16S rRNA Sequences. *Appl Environ Microb* **78:** 717-725.

Supplemental Table S1: Range of ion concentrations in the lake water.

Sampling point [h]	0	66	
Ion	concentration mmol L^{-1}		change [%]
Na^{+}	3.37×10^{3}	3.30×10^{3}	- 2
Mg^{2+}	0.38×10^{3}	0.45×10^{3}	+ 21
K^{+}	31.24	36.13	+ 16
Ca^{2+}	7.98	6.35	- 20
Sr^{2+}	0.12	0.13	+ 14
B^{3+}	0.24	0.29	+ 19
Li^{+}	0.16	0.19	+ 21
Mn^{2+}	0.004	0.012	+ 202
Cl^{-}	4.67×10^{3}	4.72×10^{3}	+ 1
SO_4^{2-}	0.12×10^{3}	0.15×10^{3}	+ 21
Br^{-}	5.85	5.56	- 5

Supplemental Table S2: Influence of ion concentrations on the lipid-derived community profile (PCoA, Figure 3a) determined via PERMANOVA. Since no significant p-values were detected, the ion concentrations appear to not influence the lipid-derived community profile.

Na^+	0.305
Mg^{2+}	0.797
K^+	0.847
Ca^{2+}	0.587
Sr^{2+}	0.433
B^{3+}	0.707
Li^+	0.329
Mn^{2+}	0.732
Cl^-	0.704
SO_4^{2-}	0.472
Br^-	0.427

Supplemental Table S3: EMIRGE reconstructed 16S rRNA sequences from all genomic datasets.

EMIRGE identifier	EMIRGE generated Organism code	Organism classification	LT2010_0.1_AM_1	LT2010_0.8_AM_1	LT2010_0.1_PM_1	LT2010_3.0_PM_1	LT2010_0.1_AM_2	LT2010_0.8_AM_2	LT2010_0.1_PM_2	LT2010_3.0_PM_2	LT2010_3.0_PM_3
1	GL982576.1	Candidatus Nanosalina	0.306648	0.022371	0.136534	0.019423	0.37111	0.040627	0.212106	0.030899	0.031587
74	AF435111.1.1471	Halobacteriaceae	0.06665	0.125015	0.102696	0.05765	0.081426	0.125955	0.14656	0.014035	0.07307
21	FN391220.1.1345	Haloquadratum	0.061292	0.126846	0.097841	0.205971	0.03888	0.121426	0.044158	0.134167	0.163772
184	AY838278.1.1473	Haloquadratum	0.025751	0.054981	0.041652	0.123513	0.013161	0.037296	0.016764	0.07613	0.092073
36	CU467230.3.1357	Haloquadratum	0.013462	0.03183	0.035136	0.081651	0.008437	0.0481	0.023456	0.084888	0.06957
268	FN391240.1.1345	Haloquadratum	0.006057	0.048996	0.040538	0.044617	0.025313	0.038762	0.047803	0.027295	0.0315
2	GL982569.1	Candidatus Nanosalinarum	0.069385	0.003875	0.032212	0.00566	0.041317	0.007582	0.030122	0.014897	0.005976
638	AJ270249.1.1461_m01	Halorubrum	0.016493	0.037364	0.015534	0.014352	0.012651	0.046263	0.030689	0.006225	0.012455
26	CU467268.2.1356	Halobacteriaceae	0.017556	0.038876	0.035013	0.036143	0.007947	0.041846	0.014409	0.03249	0.020865
17	FN393543.1.1362	Salinibacter	0.0236	0.030062	0.043557	0.031246	0.017726	0.018079	0.009464	0.023235	0.043527
20	CU467211.3.1344	Haloquadratum	0.009159	0.033432	0.024624	0.035484	0.004327	0.037572	0.012585	0.019043	0.026997
564	AY862784.1.1402	Bacteroidetes	0.005262	0.008358	0.012034	0.024879	0.013893	0.038218	0.019596	0.055355	0.061644
176	CU467143.1.1344	Halorubrum	0.021483	0.011943	0.029639	0.012409	0.011959	0.015284	0.023745	0.033542	0.01286
112	FN391263.1.1344	Halorubrum	0.002311	0.014993	0.021594	0.00761	0.016912	0.019242	0.010516	0.008107	0.00992
254	FN391293.1.1345	Halorhabdus	0.024497	0.019304	0.037433	0.006011	0.013027	0.012913	0.016954	0.005646	0.005836
107	FN391274.1.1344	Candidatus Haloredivivus	0.026788	0	0.008295	0	0.019204	0.002921	0.021214	0	0.0031
211	EF459716.1.1519	Salinibacter	0.004943	0.007906	0.010061	0.008696	0.006937	0.010766	0.008827	0.013781	0.017768
337	EU538190.1.1396	Pseudomonas	0	0	0	0	0.074523	0.002971	0.004616	0	0
179	EF533958.1.1551	Halomicrobium	0.015533	0.015592	0.012108	0.026902	0.007368	0.026459	0.025211	0.019152	0.019545

643	EF468473.1.1470_m01	Halobacteriaceae	0.023991	0.011879	0.012957	0.004094	0.014204	0.011926	0.01752	0.011946	0.010025
482	GQ282618.1.1471	Haloquadratum	0.008582	0.047589	0.010604	0.027664	0.006001	0.02702	0.009336	0.018004	0.018549
839	FN393543.1.1362_m76	Salinibacter	0.009609	0.012913	0.014118	0.015595	0.008877	0.007994	0.008607	0.020224	0.032044
140	EF690618.1.1445	Halobacteriaceae	0.003803	0.010158	0.004386	0.0068	0.00325	0.010201	0.004344	0.00433	0.007513
88	AM947502.1.1345	Halobacteriaceae	0.013599	0.03393	0.012149	0.001883	0.004137	0.012846	0.01076	0.007181	0.014389
98	CU467180.3.1354	Haloquadratum	0.007285	0.00615	0.007288	0.001965	0.006726	0.002877	0.006292	0.010914	0.004411
289	DQ432495.1.1399	Halobacteriaceae	0.003516	0.009917	0.008726	0.017261	0.014802	0.009069	0.006928	0.024406	0.014997
316	EF690563.1.1439	Halobacteriaceae	0.004727	0.012463	0.009586	0.018283	0.000671	0.010194	0.003273	0.017673	0.022148
22	EF459702.1.1440	Halomicrobium	0.008172	0.005742	0.005072	0.00281	0.002986	0.002532	0.004085	0.009141	0.003231
101	GQ282622.1.1467	Halobacteriaceae	0.003541	0.007358	0.00614	0.016151	0.007651	0.012316	0.007451	0.010752	0.01356
58	AM947497.1.1343	Halobacteriaceae	0.005455	0.00635	0.006243	0.005553	0.006678	0.007467	0.006666	0.013298	0.003301
30	CU467261.1.1348	Halobacteriaceae	0.005055	0.010734	0.011351	0.005258	0.007071	0.006368	0.002383	0.020953	0.011837
287	EU562182.1.1478	Halorubrum	0.006542	0.009091	0.004605	0.013004	0.002263	0.004192	0.012965	0.006438	0.006515
65	DQ432537.1.1395	Halobacteriaceae	0.009417	0.006287	0.005323	0.00336	0.006218	0.005213	0.003314	0.006611	0.003152
59	AM947487.1.1342	Halobacteriaceae	0.003793	0.004751	0.008137	0.001785	0.002038	0.005086	0.005545	0.006322	0.001322
44	AM947477.1.1344	Halobacteriaceae	0.006602	0.007157	0.006254	0.0029	0.001362	0.008938	0.007042	0.002696	0.00369
842	EF468473.1.1470_m34	Halobacteriaceae	0.002042	0.013332	0.004385	0.003991	0.005062	0.007432	0.011219	0.010915	0.004787
76	EU722666.1.1246	Halorhabdus	0.009702	0.006915	0.002199	0.002771	0.003374	0.004292	0.003629	0.004913	0.002159
163	EF690613.1.1440	Halobacteriaceae	0.003937	0.004909	0.003473	0.004136	0.004553	0.004693	0.004497	0.005924	0.004333
69	AM947448.1.1343	Haloquadratum	0.004414	0.01128	0.004892	0.0063	0.001959	0.005035	0.005681	0.009676	0.007598
199	AM947454.1.1343	Halobacteriaceae	0.003161	0.004988	0.005357	0.001139	0.004344	0.003413	0.003442	0	0.001561
41	CU467267.2.1356	Halobacteriaceae	0.005525	0	0.004224	0.001234	0.002986	0.002036	0.004005	0.003806	0
187	EF690583.1.1440	Halobacteriaceae	0.006621	0.005817	0.005996	0.007316	0.009781	0.007985	0.011772	0.007127	0.005184
154	CU467189.3.1357	Halobacteriaceae	0.001485	0.004869	0.003093	0.003895	0.000893	0.003066	0.00202	0.006098	0.006154
216	AY987828.1.1441	Halobacteriaceae	0.008812	0.005519	0.002134	0.007385	0.002272	0.003302	0.003485	0.011866	0.004696
841	EF459716.1.1519_	Salinibacter	0.008292	0.006016	0.004931	0.008795	0.004343	0.008146	0.003361	0.009439	0.005866

	m39										
840	FN391274.1.1344_m38	Candidatus Haloredivivus	0.004794	0	0.008491	0	0.01478	0	0.021358	0	0
19	EU722669.1.1444	Halobacteriaceae	0.002582	0	0.003254	0.002614	0.00188	0.002625	0.002557	0	0.003402
14	EF690585.1.1438	Halobacteriaceae	0.003806	0	0.00231	0.003104	0.003108	0.002523	0.001713	0	0.002526
138	FJ429313.1.1489	Haloarcula	0.001639	0	0.00259	0	0.00371	0.002575	0.005353	0	0
133	EU931577.1.1473	Haloquadratum	0.001654	0.007636	0.003299	0.004134	0.005475	0.003659	0.002238	0.009666	0.007215
208	AM947451.1.1344	Halobacteriaceae	0.000754	0	0.004241	0	0.002215	0.003906	0.001617	0.003289	0.002076
82	AM947499.1.1344	Halorubrum	0.00176	0	0.001722	0.001025	0.00132	0.003207	0.001794	0	0.001798
222	AY498650.1.1371	Haloquadratum	0.002447	0.009774	0.001934	0.002441	0.000997	0.003425	0.00132	0.006855	0.003325
180	FN391283.1.1344	Halobacteriaceae	0.002836	0.00343	0.00167	0.001347	0.001151	0.003347	0.005383	0.004678	0.002821
173	EF690565.1.1442	Halobacteriaceae	0.001661	0.00484	0.003088	0.001898	0.004045	0.002762	0.00356	0.006176	0.004452
39	AM947450.1.1345	Haloquadratum	0.001472	0.002486	0.002396	0.002512	0.001356	0.004046	0.002663	0.004678	0.002857
34	GQ282621.1.1473	Halobacteriaceae	0.001773	0	0.001723	0.002637	0.0019	0.003298	0.003446	0	0.003072
200	FN391291.1.1344	Halobacteriaceae	0.001617	0.004429	0.002394	0.001709	0	0.003445	0.002011	0.002468	0.002274
23	AM947468.1.1342	Halobacteriaceae	0.002025	0.001427	0.002203	0.001544	0.001826	0.002336	0.005155	0.004043	0
565	AM947493.1.1343	Halobacteriaceae	0.003655	0.003633	0.002091	0.001796	0.001408	0.002888	0.003105	0	0
114	AM947496.1.1351	Haloarcula	0.001757	0	0.001595	0	0.001943	0.002643	0.002672	0	0.002497
177	CU467118.3.1354	Halorubrum	0.000687	0	0.002348	0.010385	0.003647	0.002425	0.001556	0.00657	0.007983
96	FN391257.1.1346	Halorhabdus	0.001423	0	0.001181	0	0.001715	0.001971	0.004604	0	0.002181
115	AM947444.1.1348	Haloquadratum	0.003032	0.002957	0.002798	0.001093	0.0018	0.002097	0.002028	0.00611	0.002936
130	CU467153.1.1343	Halobacteriaceae	0.001588	0.001819	0.002518	0.00097	0.001949	0.001969	0.003194	0.003011	0.001601
38	FN391237.1.1353	Halobacteriaceae	0.002555	0	0.001833	0	0.003562	0	0.001038	0	0
132	FN391289.1.1340	Halobacteriaceae	0.005003	0.006247	0.000789	0.003615	0.00145	0.007636	0.00498	0	0
24	CU467116.3.1355	Halorubrum	0.002295	0.003461	0.003161	0.002153	0.001291	0.002527	0.001019	0.008199	0.00396
93	FJ172059.1.1341	Halorubrum	0.001925	0.003787	0.001853	0.003766	0.001795	0.00723	0.002496	0.016173	0.005278
235	AB012051.1.1441	Halobacteriaceae	0.001705	0.002867	0.002057	0	0.001906	0	0	0	0.00112

265	CU467142.1.1344	Halobacteriaceae	0.001485	0	0.001474	0.002248	0.000677	0	0.000573	0	0
242	CU467266.1.1348	Halobacteriaceae	0.002168	0	0.001269	0.002244	0.002095	0	0	0	0
54	AM947441.1.1346	Haloquadratum	0.001434	0.013005	0.001347	0.002055	0.002493	0.008917	0.001517	0.020319	0.004132
87	AM947456.1.1341	Halobacteriaceae	0.002139	0.001272	0.001075	0	0.001138	0.002123	0.002064	0	0
75	DQ103672.1.1407	Halogeometricum	0.001705	0	0.001391	0.001422	0.003643	0.021416	0.010615	0.010668	0.003271
221	FN391264.1.1348	Halorubrum	0	0	0.000465	0.002566	0	0	0	0	0.003485
68	CU467138.1.1341	Haloquadratum	0.001077	0.003879	0.001411	0.001197	0.001375	0.001685	0.002508	0.017033	0.00392
0	AM947471.1.1342	Halobacteriaceae	0.038747	0.024222	0.016573	0.002391	0.001665	0.002613	0.001708	0	0.002531
61	CU467214.1.1346	Haloquadratum	0.00025	0.000971	0.00058	0.002404	0.000062	0.003025	0.004699	0.005101	0.002206
161	FN391250.1.1344	Halorubrum	0	0	0.000754	0.001186	0	0.001758	0.00104	0.005423	0.001981

Supplemental Table S4. Profile of the composition of the 0.7 filter based on metagenomic analysis

Organism Type	Percent by type	Group	Percent by Group
Actinobacteria	5.78		
Bacteroidetes	0.74		
Proteobacteria	0.04	**BACTERIA**	6.56
Halobonum	0.43		
Halonotius	0.78		
Halorubrum	9.59		
Halosimplex	0.41		
Natronomonas	0.06		
Haloarcula	0.63		
Haloquadratum	20.02		
J07ABHX6 (Halobacteriales)	6.26		
J07ABHX67 (Halobacteriales)	1.11		
J07HX5 (Halobacteriales)	4.52		
J07HX64 (Halobacteriales)	3.10		
Halobacteriales (novel)	31.17		
Other Haloarchaea	9.13	**ARCHAEA (Euryarchaeota)**	87.22
Nanosalina	4.19		
Nanosalinarum	1.81		
Haloredivivus	0.22	**NANOHALOARCHAEA**	6.22
	100.00		100.00

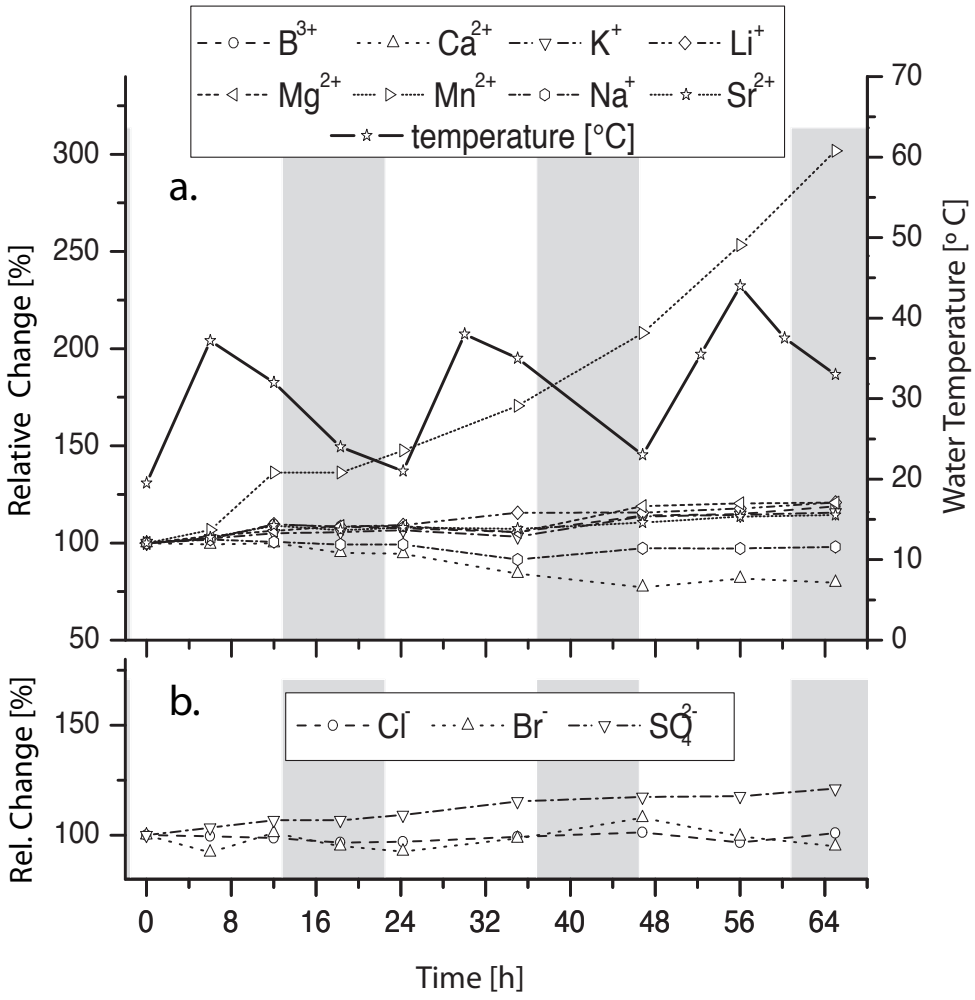

Supplemental Figure S1. Relative changes in ion concentrations during the sampling period. a) relative change in cation concentrations and lake water temperature [°C] vs. time [h] b) relative change in anion concentrations vs. time [h]. Grey areas: times without daylight.

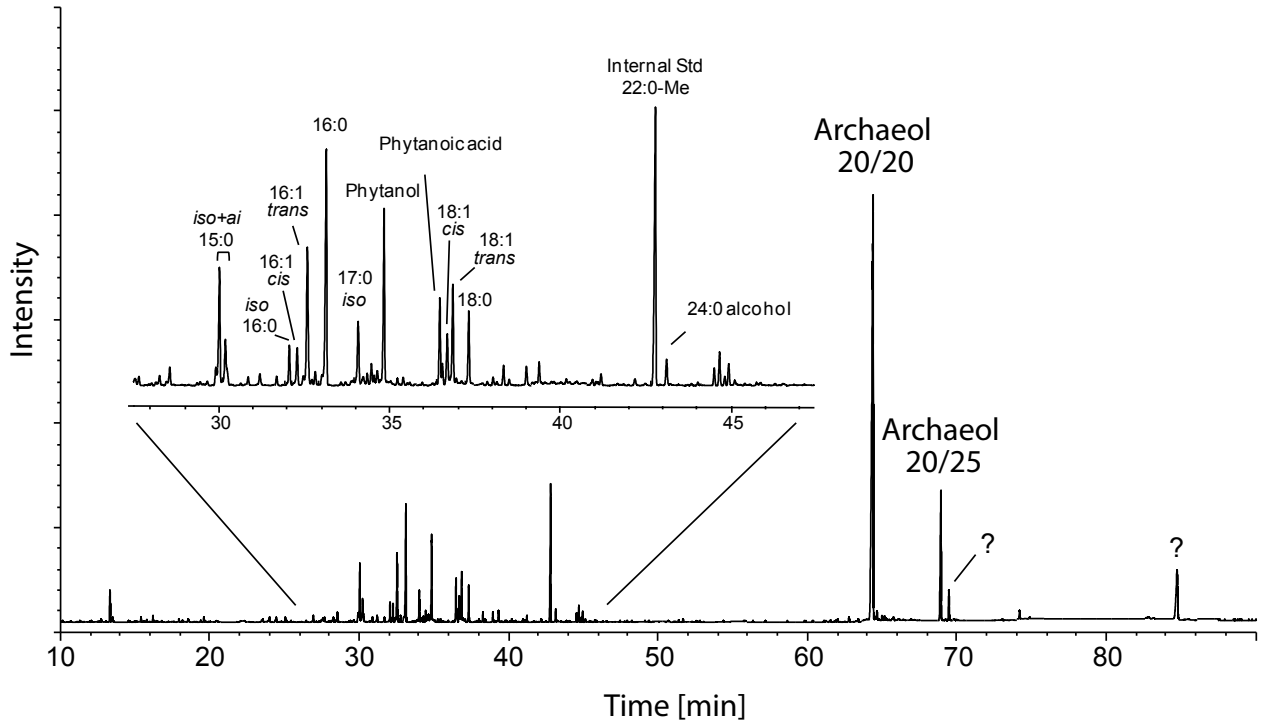

Supplemental Figure S2. Typical GC-FID chromatogram of lipids derived from alkaline hydrolysis of planktonic microorganisms in Lake Tyrrell obtained by filtration and taken at t= 0 hours.

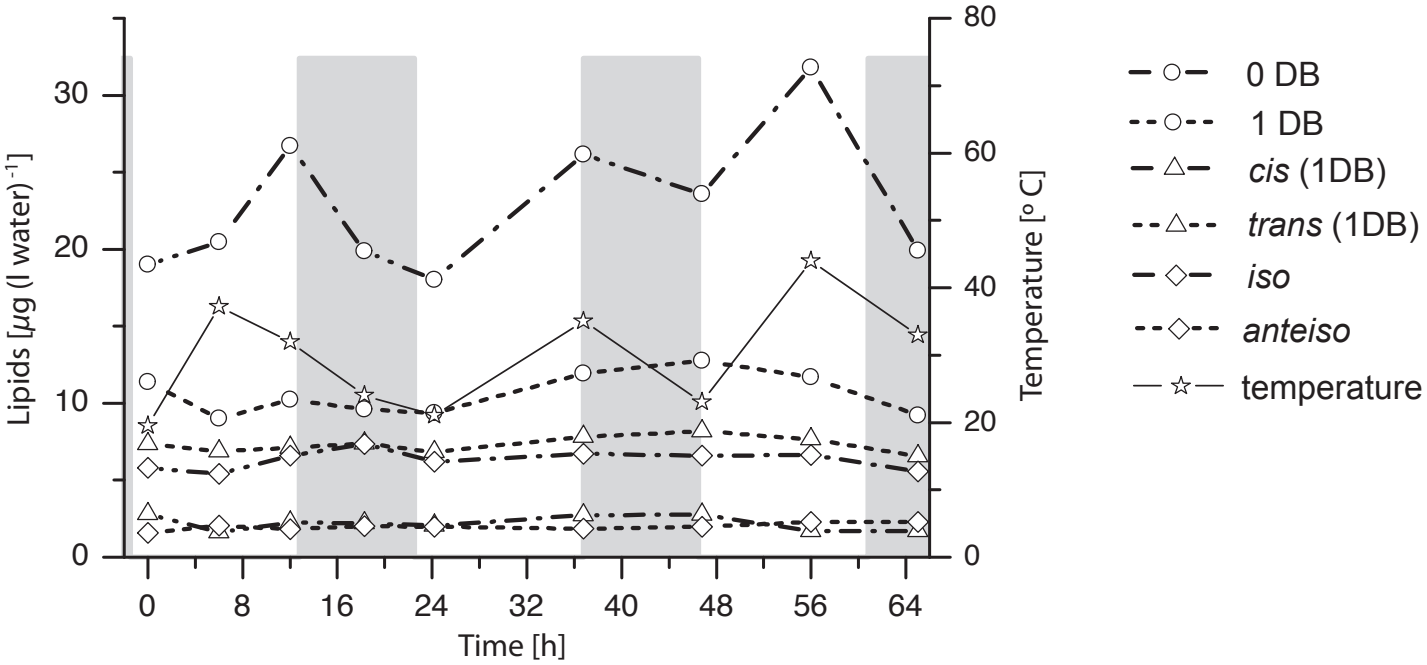

Supplemental Figure S3. Concentrations of different groups of fatty acids [µg (l lake water)-1] vs. time [h] plotted as sums of: 0 DB (iso/anteiso-C15:0, iso-C16:0, n-C16:0, iso C17:0, n-C18:0 and C17:0 2-OH fatty acids); 1 DB (cis/trans-C16:1, and cis/trans-C18:1); cis (cis-C16:1, and cis-C18:1); trans (trans-C16:1 and trans-C18:1); iso (iso-C15:0, iso-C16:0, iso-C17:0) and anteiso (anteiso-C15:0). As additional information, water temperature (stars) on each sampling point is given in °C and grey areas show hours without daylight.

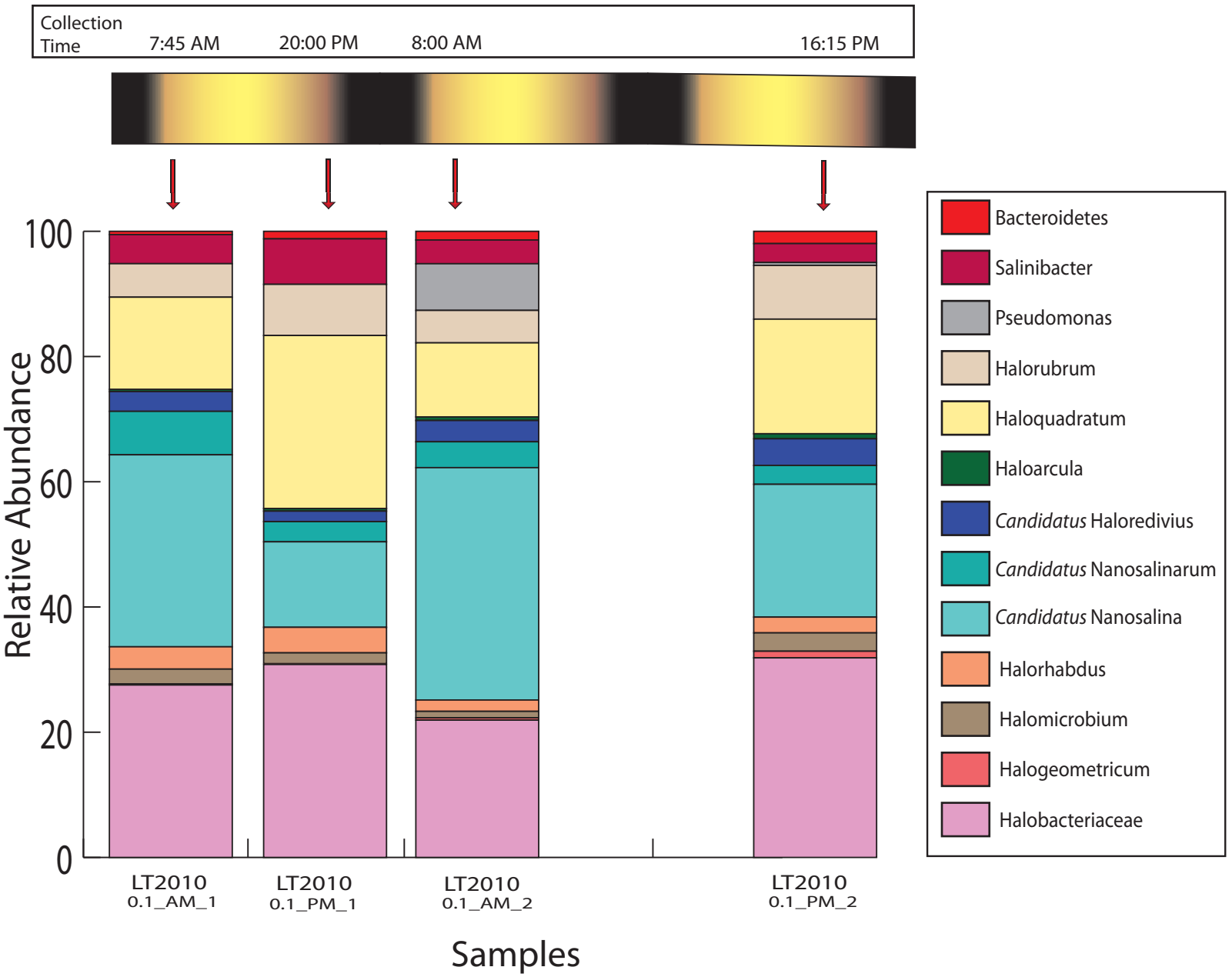

Supplemental Figure S4. Nanohaloarchaea and Halobacteria exhibit opposite relative abundance trends in 0.1 µm filter samples during a diel cycle based on reconstructed 16S rRNA abundance patterns. The relative abundances of the 12 potential OTUs defined from the 80 reconstructed 16S rRNA genes are displayed as stacked bar charts for the four time-points for which 0.1 µm filter sample datasets were available. The collection time of each sample is shown at the top, as in Figure 2. The taxonomic assignment for each OTU is limited to Genus-level, with corresponding colors depicted in the legend.